Published in: Nuclear Inst. And Methods in Physics Research B 468 (2020) 37

International Atomic Energy Agency inter-comparison of Particle Induced Gamma-ray Emission codes for bulk samples

N. Pessoa Barradas [1], J. Cruz [2], M. Fonseca [2,3], A.P. de Jesus [2], A. Lagoyannis [4], V. Manteigas [2], M. Mayer [5], K. Preketes-Sigalas [4], P. Dimitriou [1,*]

[1] International Atomic Energy Agency, Division of Physical and Chemical Sciences, Vienna International Centre, PO Box 100, A-1400 Vienna, Austria

[2] Laboratório de Instrumentação, Engenharia Biomédica e Física da Radiação (LIBPhys-UNL), Departamento de Física, Faculdade de Ciências e Tecnologia da Universidade Nova de Lisboa, Monte da Caparica, 2892-516 Caparica, Portugal

[3] Universidade Europeia, IADE, Av. Carlos I, 4, 1200-049 Lisboa, Portugal

[4] Tandem Accelerator Laboratory, Institute of Nuclear and Particle Physics, NCSR "Demokritos", 153.10 Aghia Paraskevi, Athens, Greece

[5] Max-Planck-Institut für Plasmaphysik, Boltzmannstr. 2, 85748 Garching, Germany

* Present address: Institute of Nuclear and Particle Physics, NCSR "Demokritos", 153.10 Aghia Paraskevi, Athens, Greece

PIGE has been widely used in the analysis of bulk samples, with quantification of data made usually through the use of reference samples. With a growing database of experimental cross sections becoming available, the use of first-principles data analysis methods is gaining ground. Only few codes capable of first principles analysis of PIGE data were available, but new codes have been recently developed. However, their accuracy has not been verified so far. In this work, the results of an inter-comparison of PIGE data analysis codes organised by the IAEA are presented. The inter-comparison was made through simulations for well-defined conditions, for bulk samples. Five analytical codes participated in the exercise: ERYA-Bulk, ERYA-Profiling, NDF, PiGreCo and SIMNRA. It is concluded that, although some differences are observed for some calculations, particularly in the presence of sharp resonances in the cross section, all four codes are appropriate for analysis of PIGE experimental data.

Keywords: Particle Induced Gamma Emission; Data analysis; intercomparison; NDF; SIMNRA; ERYA; PIGRECO

1. Introduction

Ion Beam Analysis (IBA) techniques such as Rutherford backscattering (RBS), Elastic Recoil Detection Analysis (ERDA), Nuclear Reaction Analysis (NRA) or Particle Induced X-ray Emission (PIXE) rely on computer codes for data analysis and quantification of the results obtained. For decades, users of the codes relied on their assumed accuracy and on tests by manual calculations that can be easily done in simple systems, such as determination of concentration and areal density from signal heights and widths or of areal density from a peak area [1]. However, validation of the codes and determination of their numerical accuracy remained an issue.

The International Atomic Energy Agency (IAEA) conducted in 2000 an inter-comparison of PIXE spectrum analysis software, with the participation of seven codes [2,3]. In this case, only the capability to retrieve peak areas was tested, and actual calculations to determine elemental concentrations from the peak areas were not included in the inter-comparison.

The IAEA organised in 2002 a technical meeting on the ‘‘Status of Software for Ion Beam Analysis in Materials Development”, which led to a review of the status of IBA particle-particle codes [4], i.e. not including techniques such as PIXE or Particle Induced Gamma-ray Emission (PIGE), and to an inter-comparison of seven particle-particle codes, including RBS, ERDA and NRA [5]. The inter-comparison included 28 theoretical calculations that tested basic calculations as well as advanced physics modelling. The inter-comparison also included four sets of experimental data. For simple ^{4}He-RBS and ^{7}Li-RBS, agreement between the NDF [6,7], RUMP [8,9] and SIMNRA [10,11] codes reached 0.3%. For ^{4}He-ERDA, agreement between NDF, RUMP and SIMNRA was 0.21%. For NRA with the D(^{3}He,p)α reaction, NDF and SIMNRA agreed within 0.2% and 0.6% for the alpha and proton yields, respectively.

In 2016, an inter-comparison of ion beam analysis software for the simulation of backscattering spectra from two-dimensional structures was presented, with four codes participating [12]. The codes were in good agreement for the single-scattering approximation and less so when plural and multiple scattering play an important role.

These inter-comparisons have led to the conclusion that the widely used particle-particle codes are compatible and provide consistent results.

For PIGE analysis, although the technique is well-established since the 1960s, a systematic inter-comparison has not yet been performed. A limited first comparison of PIGE codes was reported in 2010 [13], which included NDF, ERYA [14,15] and SPACES [16]. However, this was done in the context of thin film depth profiling using multiple complementary techniques and was not an inter-comparison aiming to validate the codes or to quantify the differences between them.

As a consequence, the technique is normally applied by comparison with well-defined standard reference materials. The potential of standardless PIGE was already stressed by the IAEA Coordinated Research Project (CRP) "Development of a Reference Database for Particle-Induced Gamma-ray Emission (PIGE) Spectroscopy" (2013-2017) [17]. However, the lack of validated PIGE analysis codes has not allowed this to be fully exploited.

This paper reports on a systematic inter-comparison of PIGE data analysis codes, initiated by the IAEA in 2018. Known existing analytical codes participated, and one code implemented PIGE for the purposes of this exercise.

2. Methodology and participating codes

Developers of PIGE codes known to calculate yields by performing first principles calculations using known physical parameters such as scattering cross sections and stopping powers, were invited to participate. The codes that were finally considered in the inter-comparison were: ERYA, with initial versions already available in 2004 [14,15] but extensively modified within the scope of the IAEA CRP on PIGE [17]; NDF [6,7], that includes PIGE since 2008 via an open

source routine, published in 2010 [13]; PiGreCo, a new code that was developed in 2016 [18]; and SIMNRA [10,11], which was extended to include a PIGE routine for the purpose of participating in the inter-comparison. Other well-known IBA codes, including Monte Carlo codes, that do not yet have PIGE implemented, were not considered. The code SPACES [16], dedicated to narrow resonance depth profiling (NRP), is directed at high resolution experiments in thin layers using isolated resonances, for which it assumes constant stopping power, and is therefore not suitable for analysis of thick bulk samples.

Two of the participating codes, NDF and SIMNRA, are IBA data analysis packages that implement a number of techniques besides PIGE. This means that they can rely on a number of methods and routines previously developed for other techniques, for instance for handling stopping power and scattering cross sections, but also for definition of sample and experimental conditions. They both participated in the IAEA inter-comparison of IBA softwares [5], where for simple cases such as ^{4}He RBS or ^{4}He ERDA with Rutherford or slowly changing cross sections, they agreed within better than 0.3% in calculation of yields and signal shapes. This was considered sufficient, since very few IBA experiments reach a 1% absolute accuracy [19]. For more advanced calculations, such as in the presence of sharp resonances, some larger differences between the two codes were observed, mainly in signal shapes due to different handling of the cross sections. However, both codes continued to be developed since that inter-comparison. The two other codes, ERYA and PiGreCo, are dedicated solely to PIGE. ERYA has two versions, ERYA-Bulk and ERYA-Profiling, which are in fact independent executable codes that share some routines. The main difference is that ERYA-Bulk only simulates bulk targets, so it does not implement energy straggling, while ERYA-Profiling includes advanced energy spread models and can simulate multi-layered targets. The current version of PiGreCo is dedicated to bulk samples only. An overview of the codes is given in Table **1**.

It was decided to concentrate the inter-comparison on calculations that all codes are, in principle and by design, capable of performing. A set of simulations for well-defined conditions and parameters was agreed on, including: reactions with slowly-changing scattering cross sections and with resonances; single element and multielemental targets; and calculations with and without the effect of beam energy spread and straggling. In all cases, the scattering angle and

scattering cross section was specified, with angular distributions assumed to be isotropic; stopping powers were specified to be taken from SRIM-2013 [20]; absorption of gamma-rays was not considered. Very importantly, it was agreed that the cross sections used in the calculations would have a threshold, i.e. they were be considered to be zero below a given energy, even if the experimental cross section included values below that given energy. Finally, in some calculations an initial yield for a pure target was given as input. All the calculations are described in detail in Table **2**.

A first set of simulations was reported by ERYA, NDF and PiGreCo. The results were compared to each other, following which SIMNRA also implemented PIGE and joined the inter-comparison exercise. The participants had the opportunity to improve the algorithms, and in this inter-comparison exercise, all codes were changed and improved as a result. The final results are presented here, since the purpose of this work is to report on the current state of the codes, including all their best capabilities.

PIGE cross sections rarely have accuracy better than 10% [21]; and therefore that is the expected minimum uncertainty in most PIGE experiments. For the purposes of this inter-comparison exercise, good agreement between codes is taken to mean that the calculations do not introduce a significant extra uncertainty in the results. We take the difference between codes to correspond to the extra uncertainty in the final quantification introduced by the use of a given code. In this sense, let us consider a rather low 5% cross section uncertainty. A 2.3% code uncertainty, added in quadrature to this 5% (assuming random uncertainties), would lead to a combined uncertainty of 5.5%, i.e. a negligible increase. We conservatively consider a 2% agreement between codes as acceptable.

If one wishes to remove the cross section uncertainty from these considerations, one could consider that very few IBA experiments have been reported at a 1% uncertainty level [19]. If such a limit would be taken, then an additional 0.5% code uncertainty would lead to a 1.1% combined uncertainty, i.e. a negligible increase.

3. Model and calculations

The underlying concepts of PIGE are simple. An energetic ion interacts with a nucleus, leading to a nuclear reaction with emission of a γ particle. The ion is often a proton and therefore the reaction is often (p,p'γ), (p,αγ) and also (p,γ). The yield coming from N_p protons with energy E interacting in a layer with areal density Nt of a given isotope species is:

$$Y(E,\theta) = \Omega(E_\gamma)\, \varepsilon_{abs}(E,E_\gamma)\, N_p\, Nt\, \sigma(E,\theta), \quad (1)$$

where $\varepsilon_{abs}(E,E_\gamma)$ is the absorption of the γ rays with energy E_γ as they travel through the sample to the detector after being generated at a depth where the beam had energy E, $\Omega(E_\gamma)$ is the absolute efficiency of the detector for γ rays with energy E_γ, and $\sigma(E,\theta)$ is the cross section for emission of a γ ray at angle θ to the incident ion direction. However, a beam with initial energy E_0 will steadily lose energy as it crosses the sample, and the total yield will be:

$$Y(E_\gamma,\theta) = \Omega(E_\gamma)\, N_p \int_0^{E0} \varepsilon_{abs}(E, E\gamma)\, Nt\, \sigma(E,\theta)/S(E)dE\,, \quad (2)$$

where S(E) is the stopping power at energy E. Note that Eq. (2) assumes that, within a given layer, the beam energy is unique and constant. In fact, this is not true; in any given layer each ion loses energy, so the beam energy decreases as the protons cross the layers.

All participating codes implement Eq. (2) (while considering $\varepsilon_{abs}(E,E_\gamma)=1$, i.e. no absorption of the gamma rays), but they do so in different ways, which can lead to differences in the calculated values. For instance, often the areal density of sub-layers is taken to be sufficiently small such that cross section and stopping power are considered to be constant within the sub-layer. However, in a given sub-layer, the cross section and stopping power can be taken as the value on top or bottom of the layer, the average of those two values, or they can be integrated over the sub-layer. The calculated yield will be different depending on the option taken.

Furthermore, at a given depth the beam energy is not unique due to beam energy spread and energy straggling; the beam has an energy distribution Γ. The most important effect for PIGE is that, in a given layer, the effective interaction cross section is [22,23]

$$\sigma_{eff}(E,\theta) = \int_{-\infty}^{+\infty} \Gamma(E',\theta)\sigma(E-E',\theta)dE'), \quad (3)$$

In cases where the cross section changes quickly with energy, the effective cross section in a given layer can be very different than the cross section for the average beam energy in the layer - up to one order of magnitude in multilayers in cases constructed to maximize the effect [22]. In bulk samples the effect is much lower, but can be significant near resonances in the cross section, whenever the beam energy spread is comparable to the resonance width. Not all participating codes implement Eq. (3), as detailed below for each code.

In summary, the most important points that influence calculated yields are: the handling of stopping power, interaction cross sections and of energy straggling; how the target is divided in internal sub-layers for calculation purposes; and how calculations are made within one sub-layer.

In this section, some calculation details are given for each participating code. Further details can be found in the publications dedicated to each code [6,7,10,11,14,15,18].

3.1. ERYA-Bulk

ERYA-Bulk evaluates the yield taking the whole bulk sample and evaluating the integral of Eq. (2), using a constant energy step that is defined by the user. For calculation 1-a, different energy steps were used (from 0.01 keV to 200 keV) and no differences on the yield were obtained, which shows that the calculation is stable and that, for smooth varying cross sections, it does not depend on the definition of internal sub-layers.

ERYA-Bulk uses SRIM stopping powers. When a stopping power is needed for a given energy, linear interpolation from the two nearest tabulated values is used. This program evaluates the

cross section at a given energy by performing also a linear interpolation from the two nearest excitation function tabulated values.

ERYA-Bulk takes the initial and final energy of each interval step to evaluate the stopping power, which is taken as the arithmetic average of the two boundaries values.

Inside each sub-layer the cross-section is evaluated by integrating the cross section tabulated data via an Adaptative Integration Method (Trapezoidal Method).

A stability test was made by calculating case 1 for constant stopping power and constant cross section. In this case, in principle the yield should be linear with beam energy. The cross section was set to 1 mb above 3 MeV and 0 below. Calculations were made for two different values of the stopping power, 1.2 and 1.77 eV/(10^{15} at./cm^2). The maximum deviation from linearity was 0.23%, being below 0.1% in most cases.

3.2. ERYA-Profiling

ERYA-Profiling is capable of calculating multi-layered samples. Each real layer is split in equal sub-layers of constant areal density, whose value is user-defined.

ERYA-Profiling shares the same functions and routines from ERYA-Bulk to calculate stopping powers and cross sections, with the minor exception that the stopping power tables for ERYA-Profiling adds the elemental densities and mean ionization potentials to the original ERYA-Bulk database files.

ERYA-Profiling evaluates the yields with Eq. (2), taking for the energy distribution function $\Gamma(E', \theta)$ the convolution of three dispersion distributions (thermal, resolution and straggling) around the initial beam energy at the beginning of each sub-layer.

Once completed each layer (with constant density), the energy losses are computed from a formula that depends on the stopping-power and updates the new beam energy for the next layer.

The integration will continue until the last sub-layer is reached or when the energy beam drops to zero.

Given that ERYA-Profiling is designed for calculations with energy spread, the stability test for case 1, which does not include energy spread, was not made.

3.3. NDF

By default, NDF subdivides a bulk sample into internal sub-layers of equal areal density. This is the main integration step. The energy loss in each internal layer is different; therefore the internal layers do not have equal energy width. The actual areal density of the internal layers is problem-dependent, determined by NDF from the stopping power. For calculation 1, the default value was 1000×10^{15} at./cm^2. This value can be user-defined; by decreasing or increasing it one order of magnitude, the maximum difference in calculated yield was found to be 0.003%, which shows that the calculation is stable and does not depend critically on the definition of internal sub-layers.

NDF uses SRIM stopping powers in the following way. SRIM is used to calculate 5000 stopping power values covering the required energy range. When a stopping power value is needed for a given energy, linear interpolation on these 5000 values is made. To calculate the energy loss in a sub-layer, the stopping power is integrated over the beam energy within the layer, using a simple Simpson rule. Because the stopping power changes slowly, this is accurate for the sub-layer areal density values used in NDF.

Linear interpolation is made between tabulated values of cross section. The cross section is always integrated in each sub-layer, thus avoiding the need for very thin layers. Furthermore, by default NDF convolutes the cross section with the energy spread of the beam according to Eq. (3) whenever straggling is calculated.

NDF implements different straggling models. For this exercise, Bohr straggling was used in the required calculations and the Tschalär effect [24], which is calculated by default in NDF, was not included in the calculation.

The stability test for constant stopping power and constant cross section was also made, showing a maximum 0.0007% deviation from linearity. This is within the expected accuracy of single precision real numbers used in NDF.

3.4. PiGreCo

The code treats bulk samples by dividing them into equally energy-spaced sub-layers. The default value of the energy step is determined by the minimum energy step in the corresponding cross section to be used, but it can be also user defined if a different one is desired. The value used for the comparison calculations of the current work was set to 1 keV.

The stopping power for each sub-layer is calculated at the middle of the layer. In its current version PiGreCo implements two ways for calculating the stopping power at a given energy: either by using the well-known Ziegler, Biersak and Littmark [25] compilation or by using SRIM stopping powers. For SRIM calculations, the code uses as input tabulated values for a proton energy range between 10 keV to 20 MeV for each element between Z = 1 to 92. The stopping power at the desired energy is then calculated by a simple linear interpolation between the existing points. In the case of composite target materials, the Bragg rule is used.

Cross sections are read directly from R33 formatted files in a tabulated form. The cross section corresponding to a specific energy is determined by a linear interpolation between known values. The inclusion of straggling in the yield calculation is user selectable. In the simple case where no straggling is selected, the cross section used is the one corresponding to the energy at the middle of the sub-layer. In the straggling inclusion case, Bohr straggling is used and is convoluted with the energy spread implemented in Eq. (3).

A stability test was performed for constant cross section and constant stopping power which in the worst case resulted in a 0.23% divergence from linearity.

3.5. SIMNRA

In the case of PIGE simulations SIMNRA subdivides a bulk sample into internal sub-layers with thicknesses so that the energy loss in each sub-layer is close to the FWHM of the energy spread of the incident particle beam. Alternatively the sub-layer thicknesses can be chosen to provide about constant energy losses in each sub-layer, the desired energy-loss is user defined.

SIMNRA uses SRIM stopping powers in the following way: SRIM is used to calculate 840 logarithmically spaced stopping power values from 1 keV to 50000 keV. The stopping power for a specific energy is obtained by linear interpolation of these values. The energy-loss in a sub-layer is obtained by solving the differential equation $S(E) = -dE/dx$ (with $E(x)$ the mean beam energy in a given depth x and $S(E)$ the energy-dependent stopping power) using a fifth order Runge-Kutta method with embedded fourth order Runge-Kutta with Cash-Karp parameters [26] for an error estimate and automatic step width control of the energy-loss calculation. The accuracy of the energy-loss calculation is of the order of a few times 10^{-6}, i.e. for energy losses of the order of 1 MeV the inaccuracy is only a few eV.

Tabulated cross-section values are linearly interpolated. The cross section is always integrated in each sub-layer and is convoluted by default with the energy spread of the beam according to Eq. (3). SIMNRA implements different straggling models, for this exercise Bohr straggling was used when required. The Tschalär effect [24] cannot be switched off and was always included in the calculations if straggling was considered.

The stability test with constant stopping power and constant cross section showed a maximum deviation from linearity of about 10^{-10}%.

4. Results and discussion

The yield as a function of beam energy often changes several orders of magnitude in the examples chosen. For the purposes of comparing the results of the different codes, all results were normalised to the average of the values calculated by all codes: first, the average value of the simulations done by the different codes was calculated. Then, the ratio between each code and that average was calculated. It is this ratio that is presented, except where otherwise noted.

4.1. Slowly changing cross section, monoelemental target, no energy spread

Simulation 1-a corresponds to the simplest case tested in this inter-comparison. The $^{10}B(p,p'\gamma)^{10}B$ reaction, with emission of a 718 keV γ, was chosen because the cross section (Lagoyannis et al. 2015 [27]) changes slowly with energy. The cross section, shown in Figure 1, was truncated to zero at 3 MeV. A pure boron target was considered, which simplifies stopping power calculations. Beam energy spread and straggling were not included in the calculation. Finally, calculations were made from 3 to 5 MeV initial beam energy, at 200 keV steps.

The yields calculated by all codes are shown in Figure 2a). It is clear that the agreement is excellent, but details are difficult to observe. The ratio of the codes to the average of all simulations is shown in Figure 2b). Agreement is better than 0.6% in all cases. The ratio to average values for ERYA-Bulk are lower in the low energy range close to 3 MeV, approaching values for the other codes at higher energies. This initial difference may be due to the way the cross section is truncated at 3 MeV by the different codes. In fact, the difference in yield between ERYA-Bulk and the other codes is lowest at low energies in absolute terms (counts), but given the low yield at low energies, it becomes higher in relative terms (ratio). This agreement is similar to what was obtained for RBS and ERDA [5]. Agreement is 0.01% or better between NDF, PiGreCo and SIMNRA, which is extremely good and better than what was obtained for e.g. NDF and SIMNRA in RBS and ERDA [5].

4.2. Slowly changing cross section, multielemental target, no energy spread

Simulation 1-b is equal to 1-a, but with a multielemental target where boron is only 10 at.%. The results are shown in Figure 3 and are very similar to those of calculation 1-a; all codes agree

within a maximum difference of 0.6%. As in calculation 1-a, the values calculated by ERYA-Bulk near 3 MeV are lower than those calculated by the other codes and become less different at higher energies.

The difference between NDF, PiGreCo and SIMNRA is within 0.025%, with NDF below the other two codes. One should keep in mind that in the IAEA inter-comparison of RBS and ERDA codes for the simplest problems, differences in yield of up to 0.3% between NDF and SIMNRA were found. The current results are one order of magnitude closer, and it is highly unlikely that any PIGE experiment will ever approach a total 0.025% uncertainty (or even 0.6%), even excluding systematic uncertainties such as that coming from the cross section.

4.3. Slowly changing cross section, monoelemental target, defined initial yield, no energy spread

Simulation 2-a-i is for a different reaction, $^{10}B(p,\alpha\gamma)^{7}Be$, with emission of a 429 keV γ, calculated at 100 keV intervals between 3 and 3.8 MeV. The cross section for this reaction, shown in Figure 4, also changes slowly with energy, with no sharp resonances. A pure boron target was considered, and beam energy spread and straggling were not taken into account. The cross section is taken from [27] and is truncated to zero at 3 MeV. In this calculation, it was considered that a known yield exists for boron at 3 MeV, of 580000 counts. This yield is supposed to account for the cross section at energies below 3 MeV.

The results for all codes are shown in Figure 5. All results agree within better than 0.3%. As in the previous cases, the ERYA-Bulk result is lower than the other codes near the origin, becoming progressively similar to the other results with higher initial beam energy. Agreement is 0.004% or better between NDF, PiGreCo and SIMNRA. This is extraordinarily good agreement.

A similar calculation, but for the $^{10}B(p,p'\gamma)^{10}B$ reaction between 3 and 3.8 MeV (simulation 2-b-i), led to agreement within 0.11% between all codes and within 0.04% between NDF, PiGreCo and SIMNRA, as shown in Figure 6.

4.4. Slowly changing cross section, multielemental target, defined initial yield, no energy spread

Simulation 2-a-ii is equal to 2-a-i, but with a multielemental target where boron is only 10 at.%. The results are shown in Figure 7. All codes agree within 0.3%. As in the previous cases, ERYA-Bulk shows the largest difference at low energy.

Agreement between NDF, PiGreCo and SIMNRA is within 0.04%. Note that at the origin, for a 3 MeV initial beam energy, there is some difference in the calculated value, with the curve for SIMNRA results lying slightly below those for NDF and PiGreCo. This difference is due to the way the initial yield is calculated. In fact, the initial yield 580000 counts is given for a pure boron target. For a multielemental target, this yield has to be normalised to boron concentration and to the ratio of stopping power in boron and in the actual material (B 10 O 40 Fe 50). An accurate calculation would require knowledge of the shape of the cross section below the 3 MeV threshold, which is not available. Therefore, different implementations make different assumptions, and it is not possible to say which method is preferable. All in all, the 0.04% agreement at 3 MeV (which includes ERYA-Bulk) must be considered excellent.

A similar calculation, but for the $^{10}B(p,p'\gamma)^{10}B$ reaction between 3 and 3.8 MeV (simulation 2-b-ii), led to agreement within 0.08% between all codes and within 0.05% between NDF, PiGreCo and SIMNRA , as shown in Figure 8.

These six calculations demonstrate that, for simple cases where the cross section changes slowly and straggling is not considered, all participating codes agree within better than 0.6%, which is similar what was obtained in the IAEA inter-comparison of IBA particle codes for RBS and ERDA [5]; considering NDF, PiGreCo and SIMNRA, agreement is around 0.1%.

4.5. Cross section with resonances, no energy spread

Simulation 3-a is for the $^{19}F(p,p\gamma_2)^{19}F$ reaction, with emission of a 197 keV γ. This reaction was chosen because the cross section, shown in Figure 9 (Jesus et al. 2000 [28]), has a number of

sharp resonances. A pure fluorine target was considered. Beam energy spread and straggling were not included. Calculations were made at 1 keV steps between 1 and 2.8 MeV. The cross section was truncated to zero at 1 MeV. Note that this very narrow energy step is not realistic, as it would not be used in a real experiment. It was used to allow comparison of details in the calculations.

The results for all codes and for the entire energy range are shown in Figure 10a). Despite the visible differences in the calculations, agreement between all codes is better than 0.25% in the entire energy range, which is much better than the accuracy of any PIGE experiment so far reported (or, for that matter, any RBS experiment).

The results are shown in selected energy ranges in Figure 10b) to Figure 10e). In the first 10 keV above the threshold, in the energy range 1000-1010 keV (Figure 10b), the differences between codes are below 0.25%. In any case, in this range the yields are very low, and this relative difference corresponds to absolute differences below 0.2 counts, which is not significant.

Figure 10c) shows the data calculated at energies around the 1093 keV sharp resonance. All codes agree within 0.15%. PiGreCo seems to show a small relative increase in yield with a large slope at the onset of the resonance, followed by an equally small and steep decrease, within 2 to 3 keV. The same energy range is shown in Figure 10d), but the yield differences relative to NDF are plotted. These reach ±6 counts at 1100 keV, for which the yield is around 20000 counts. The associated statistical uncertainty, if this were experimental data, would be around 140 counts. Again, this shows that the uncertainty due to the code used is well below expected experimental uncertainties. It is interesting to note that PiGreCo and SIMNRA results vary in a similar way and ERYA-Bulk results vary by approximately the same amount but towards negative values. As stated before, it is not possible to say which code is correct.

The results obtained at energies around the group of resonances at 1349, 1376 and 1425 keV, which are less sharp than that at 1093 keV, are shown in Figure 10e). The codes agree within 0.04% in this energy range. Note that NDF seems to display very small fluctuations, around

0.001% in the 1 keV range. These are very likely due to the single precision real numbers used in NDF.

The results for simulation 3-b, made for exactly the same conditions but for a multielemental target, with composition ^{nat}F 10 O 30 Cr 60, are shown in Figure 11. The results are nearly identical to those of simulation 3-a, with maximum deviation between codes below 0.25%.

4.6. Slowly changing cross section, with energy spread

The calculation presented here, case 4-1-a. is equal to that presented in section 4.1, 1-a, but in this case 3 keV beam energy spread and Bohr straggling were included in the calculations.

The cross section is, as mentioned above, truncated to zero at energies below 3 MeV. In this case, in the absence of beam energy spread, the yield will be exactly zero for a 3 MeV initial beam energy. This was calculated by all codes in case 1-a. However, in the presence of beam energy spread, assumed to be Gaussian-shaped, exactly half the beam particles have energy above 3 MeV, for which the cross section is above zero. In this case, a small but non-zero yield will be calculated. The yield at 3 MeV calculated by ERYA-Profile, NDF, PiGreCo and SIMNRA are 48.9, 64.5, 44.4 and 65.0 counts. As truncated cross sections are an artificial construct, these differences are not significant. As a comparison, the yield at 5 MeV is over 6.1 million counts.

The results for all codes are shown in Figure 12. All codes agree within 0.3%, and NDF and SIMNRA are nearly undistinguishable.

The results for the same conditions but in a multielemental target (simulation 4-1-b) are very similar. In fact, there are no reasons to expect that energy spread should lead to different behaviour in calculations made for mono- or multielemental bulk targets.

For the calculations with given yield at the threshold energy (4-2-a-i, 4-2-a-ii, 4-2-b-i, 4-2-b-ii), the large initial yield is added to the small calculated yield for the threshold energy, which masks

the effect of the beam energy spread. In all those calculations, the codes agree within 0.2%, with NDF and SIMNRA agreeing within 0.02%.

4.7. Cross section with resonances, with energy spread

The calculation presented here, case 4-3-a. is equal to that presented in section 4.5, 3-a, but with 3 keV beam energy spread and Bohr straggling included in the calculations. This is the most demanding calculation defined in the inter-comparison. At the threshold energy, 1 MeV, the beam energy spread leads to a non-zero calculated yield, which is 20.8, 11.1, 8.9 and 11.1 counts for ERYA-Profile, NDF, PiGreCo and SIMNRA, respectively. As for calculation 4-1-a above, these differences are not significant.. One should also note that for this simulation the yield for the maximum beam energy 2.7 MeV is around 9.5 million counts.

The results are shown in Figure 13a) and b) for all codes. At the lower energies the result curves for ERYA-Profile and PiGreCo converge from values around 15% different from NDF and SIMNRA to values around 1% different at 1020 keV for PiGreCo and at 1050 keV for ERYA-Profile.

Around the 1093 keV resonance, results for ERYA-Profile and PiGreCo deviate strongly from NDF and SIMNRA. The results are shown in absolute value in Figure 13c), where it is clear that the observed differences must be due to the way the energy spread is handled by the codes. ERYA-Profiling leads to a calculated signal that is broader than NDF and SIMNRA at the high energy side of the resonance, while PiGreCo leads to a signal that is less broad than NDF and SIMNRA at the low energy side of the resonance. The difference is around 0.5 keV, which experimentally would be extremely difficult to observe. All in all, the large relative differences in the calculations do not arise from large differences in the yields calculated, but from the differences in calculated shape (energy width).

At energies above 1120 keV, the differences between the codes are within 1%. NDF and SIMNRA results are practically the same. ERYA-Profile and PiGreCo behave in a similar way, (Figure 13b), but clearly different from NDF and SIMNRA. In any case, the difference is

quantitatively within acceptable bounds; it can be concluded that, even in this demanding case, all participating codes are fit for the purpose of analysing experimental PIGE data.

The largest difference between NDF and SIMNRA, observed at low energies, is below 0.15%. It is noted that the ratio of SIMNRA to NDF presents a wave-like ripple. This ripple is not present in the ratios of ERYA-Profile and PiGreCo to NDF, which leads to the conclusion that it is likely due to the internal division of sub-layers in the SIMNRA code. The maximum amplitude is 0.02%, much below any detectable signal.

NDF and SIMNRA also present some differences near the 1093 keV sharp resonance. The maximum relative difference is however below 0.1%, which at this level of detail must be considered extraordinarily good agreement.

5. Conclusions

The IAEA organized the first systematic inter-comparison exercise of PIGE data analysis codes for bulk samples. Existing PIGE analytical codes participated, and other codes in active development, including analytical and Monte Carlo codes, were invited to participate. One of those codes under development implemented the technique and then participated. In total, five codes capable of first-principles analysis of PIGE data participated in this inter-comparison exercise: ERYA-Bulk, ERYA-Profiling, NDF, PiGreCo and SIMNRA.

A set of four exercises (some comprising sub-exercises) was defined by the participating code developers to test the performance of the codes on bulk analysis, starting from smooth cross sections and simple elemental compositions, then extending the exercise to cross sections with sharp resonances, including effects such as beam energy spread and straggling. The cross sections and stopping powers used, as well as details of the calculations, were agreed by the participants. The defined calculations included three different reactions, and concentrated on:

1. Smooth cross sections known down to the threshold energy (no beam energy spread)
2. Smooth cross section known down to a given energy (no beam energy spread)

3. Cross section with sharp resonance (no beam energy spread)
4. Straggling added to cases 1 to 3 using Bohr's model with a beam energy spread of 3 keV

Both monoelemental and multielemental targets were considered. Some of the exercises had a very fine energy step. Altogether, the calculations allowed to test the main issues affecting calculation of PIGE data for bulk target. Multilayered targets were not addressed.

When beam energy spread and straggling are not included in the calculations, all codes agreed with differences that reached a maximum of 0.6%, but which were generally below 0.3%. This is much below the uncertainty of the experimental cross sections used for PIGE, seldom below 5 to 10% and often larger [21]. In the absence of sharp resonances, NDF, PiGreCo and SIMNRA agree within 0.05%. In the presence of a cross section with sharp resonances, ERYA, NDF, PiGreCo and SIMNRA agree within 0.25%.

When beam energy spread and straggling are included in the calculations, differences in the calculated yields up to 20% were observed. However, we note that such large differences were confined to the vicinity of very sharp resonances, where the different implementation by the codes of the calculation of energy spread and straggling, as well as the numerical integration method, leads to a different shape of the energy-dependent yield (broader or less broad). In this case, it is the shape of the increase of the PIGE yield with beam energy that is the real difference between the codes, and the large relative differences in yield for one given beam energy are not significant; a sizeable part of this effect seems to be due to a shift in the energy axis of less than 0.5 keV.

When only NDF and SIMNRA are considered, the maximum difference is 0.2%. Given the complexity of the case, this must be considered excellent agreement.

In summary, all participating codes are fit for the purpose of analysis experimental PIGE data. In general, agreement between the codes is much better than the accuracy of available cross sections.

We note that these conclusions are valid for bulk samples only. For multilayers, particularly in the presence of thin layers and cross sections with sharp resonances, it is expected that the handling of straggling and numerical integrations will play a larger role. This will be the object of a future study.

References

1. Wei-Kan Chu, James W. Mayer, and Marc-A. Nicolet, Backscattering Spectrometry, Academic Press, New York, 1978.
2. Inter-comparison of PIXE spectrometry software packages, International Atomic Energy Agency TECDOC No. 1342 (2003), Vienna. ISBN:92–0–101203–9.
3. M. Blaauw, J.L. Campbell, S. Fazinic, M. Jaksic, I. Orlic, P. Van Espen, Nuclear Instruments and Methods in Physics Research B 189 (2002) 113.
4. E. Rauhala, N.P. Barradas, S. Fazinic, M. Mayer, E. Szilágyi, M. Thompson, Nuclear Instruments and Methods in Physics Research B 244 (2006) 436.
5. N.P. Barradas, K. Arstila, G. Battistig, M. Bianconi, N. Dytlewski, C. Jeynes, E. Kótai, G. Lulli, M. Mayer, E. Rauhala, E. Szilágyi, M. Thompson, Nuclear Instruments and Methods in Physics Research B 262 (2007) 281.
6. N.P. Barradas, C. Jeynes, and R.P. Webb, Applied Physics Letters 71 (1997) 291-293.
7. N.P. Barradas, C. Jeynes, Nuclear Instruments and Methods in Physics Research B 266 (2008) 1875.
8. L.R. Doolittle, Nuclear Instruments and Methods in Physics Research B 9 (1985) 344.
9. L.R. Doolittle, Nuclear Instruments and Methods in Physics Research B 15 (1986) 227.
10. M. Mayer, AIP Conf. Proc. 475 (1999) 541.
11. M. Mayer, Nuclear Instruments and Methods in Physics Research B 332 (2014) 176.
12. M. Mayer, P. Malinský, F. Schiettekatte, Z. Zolnai, Nuclear Instruments and Methods in Physics Research B 385 (2016) 65.

13. N.P. Barradas, R. Mateus, M. Fonseca, M.A. Reis, K. Lorenz, I. Vickridge, Nuclear Instruments and Methods in Physics Research B 268 (2010) 1829.

14. R. Mateus, A.P. Jesus, J.P. Ribeiro, Nuclear Instruments and Methods in Physics Research B 219 (2004) 519.

15. R. Mateus, A.P. Jesus, M.Fonseca, H.Luís, J.P. Ribeiro, Nuclear Instruments and Methods in Physics Research B 264 (2007) 340.

16. I. Vickridge, G. Amsel, Nuclear Instruments and Methods in Physics Research B 45 (1990) 6.

17. Development of a Reference Database for Particle Induced Gamma Ray Emission (PIGE) Spectroscopy, International Atomic Energy Agency TECDOC No. 1822 (2017), Vienna. ISBN:978-92-0-106317-5.

18. K. Preketes-Sigalas, A. Lagoyannis, M. Axiotis, Proc. 25th Hellenic Conference on Nuclear Physics, 3-4 June 2016, p. 162.

19. C.Jeynes, N. P.Barradas, E. Szilagy, Analytical Chemistry 84 (2012) 6061.

20. J.F. Ziegler, J.P.Biersack, and M.D.Ziegler, SRIM - The Stopping and Range of Ions in matter, Maryland, SRIM Co., 2008. <www.srim.org>

21. IAEA Ion Beam Analysis Nuclear Data Library (IBANDL), <https://www-nds.iaea.org/exfor/ibandl.htm>.

22. N.P. Barradas, E. Alves, C. Jeynes, M. Tosaki, Nuclear Instruments and Methods in Physics Research B 247 (2006) 381.

23. N.P. Barradas, E. Alves, Nuclear Instruments and Methods in Physics Research B 249 (2006) 796.

24. C. Tschalär, Nuclear Instruments and Methods 61 (1968) 141.

25. J.F. Ziegler, J.P. Biersack, U. Litmark, The Stopping and Range of Ions in Matter, Pergamon Press, New York, 1985.

26 W.H. Press, B.P. Flannery, S.A. Teukolsky, and W.T. Vetterling. Numerical Recipes,

Cambridge University Press, Cambridge, New York, 1988.

27. A. Lagoyannis, K. Preketes-Sigalas, M. Axiotis, V. Foteinou, S. Harissopulos, M. Kokkoris, P. Misaelides, V. Paneta, N. Patronis, Nuclear Instruments and Methods in Physics Research B 342 (2015) 271.

28. A.P. Jesus, B. Braizinha, J.P. Ribeiro, Nuclear Instruments and Methods in Physics Research B 161-163 (2000) 186.

Table 1. Summary of codes.

Code and version	Status	Programming language	Distribution	Source code	Real number precision
ERYA-Bulk	Active development	C++ wxWidgets (GUI)	Freeware	Restricted to author.	Double
ERYA-Profiling	Active development	C++ wxWidgets(GUI)	Freeware	Restricted to author.	Double
NDF v9.7a	Active development	Fortran / C PIGE is Fortran	Commercial. PIGE routine open source	Restricted to author. PIGE routine open source	Single
PiGreCo	Active development	C++, Qt libraries	Free	Free	Double
SIMNRA 7.02	Active development	Delphi	Commercial	Restricted to author	Double

Table 2. Calculations.

#	Energy range (MeV)	Energy step (keV)	Reaction	E_γ (keV)	θ (º)	Target (at.%)	Cross section	Energy spread [1]	Initial yield (Nγ/sr/μC)
1-a	3-5	200	$^{10}B(p,p'\gamma)^{10}B$	718	165	^{nat}B 100	Lag2015	No	No
1-b	3-5	200	$^{10}B(p,p'\gamma)^{10}B$	718	165	^{nat}B 10 O 40 Fe 50	Lag2015	No	No
2-a-i	3-3.8	100	$^{10}B(p,\alpha\gamma)^{7}Be$	429	150	^{nat}B 100	Lag2015	No	580000 [2]
2-a-ii	3-3.8	100	$^{10}B(p,\alpha\gamma)^{7}Be$	429	150	^{nat}B 10 O 40 Fe 50	Lag2015	No	580000 [2]
2-b-i	3-3.8	100	$^{10}B(p,p'\gamma)^{10}B$	718	165	^{nat}B 100	Lag2015	No	580000 [2]
2-b-ii	3-3.8	100	$^{10}B(p,p'\gamma)^{10}B$	718	165	^{nat}B 10 O 40 Fe 50	Lag2015	No	580000 [2]
3-a	1-2.7	1	$^{19}F(p,p\gamma_2)^{19}F$	197	130	^{nat}F 100	Jes2000	No	No
3-b	1-2.7	1	$^{19}F(p,p\gamma_2)^{19}F$	197	130	^{nat}F 10 O 30 Cr 60	Jes2000	No	No
4-1-a	3-5	200	$^{10}B(p,p'\gamma)^{10}B$	718	165	^{nat}B 100	Lag2015	Yes	No
4-1-b	3-5	200	$^{10}B(p,p'\gamma)^{10}B$	718	165	^{nat}B 10 O 40 Fe 50	Lag2015	Yes	No
4-2-a-i	3-3.8	100	$^{10}B(p,\alpha\gamma)^{7}Be$	429	150	^{nat}B 100	Lag2015	Yes	580000 [2]
4-2-a-ii	3-3.8	100	$^{10}B(p,\alpha\gamma)^{7}Be$	429	150	^{nat}B 10 O 40 Fe 50	Lag2015	Yes	580000 [2]
4-2-b-i	3-3.8	100	$^{10}B(p,p'\gamma)^{10}B$	718	165	^{nat}B 100	Lag2015	Yes	580000 [2]
4-2-b-ii	3-3.8	100	$^{10}B(p,p'\gamma)^{10}B$	718	165	^{nat}B 10 O 40 Fe 50	Lag2015	Yes	580000 [2]
4-3-a	1-2.7	1	$^{19}F(p,p\gamma_2)^{19}F$	197	130	^{nat}F 100	Jes2000	Yes	No
4-3-b	1-2.7	1	$^{19}F(p,p\gamma_2)^{19}F$	197	130	^{nat}F 10 O 30 Cr 60	Jes2000	Yes	No

Lag2015: A. Lagoyannis et al., NIMB 342 (2015) 271-276, truncated to 0 below 3 MeV.
Jes2000: A.P. Jesus et al., Nucl. Instr. Meth. B 161-163 (2000) 186, truncated to 0 below 1 MeV.
[1] Energy spread includes 3 keV beam energy spread and Bohr straggling.
[2] Yield for a 3 MeV proton beam on a pure Boron reference target.

Figure 1. Cross section for reaction $^{10}B(p,p'\gamma)^{10}B$ at 165° [27].

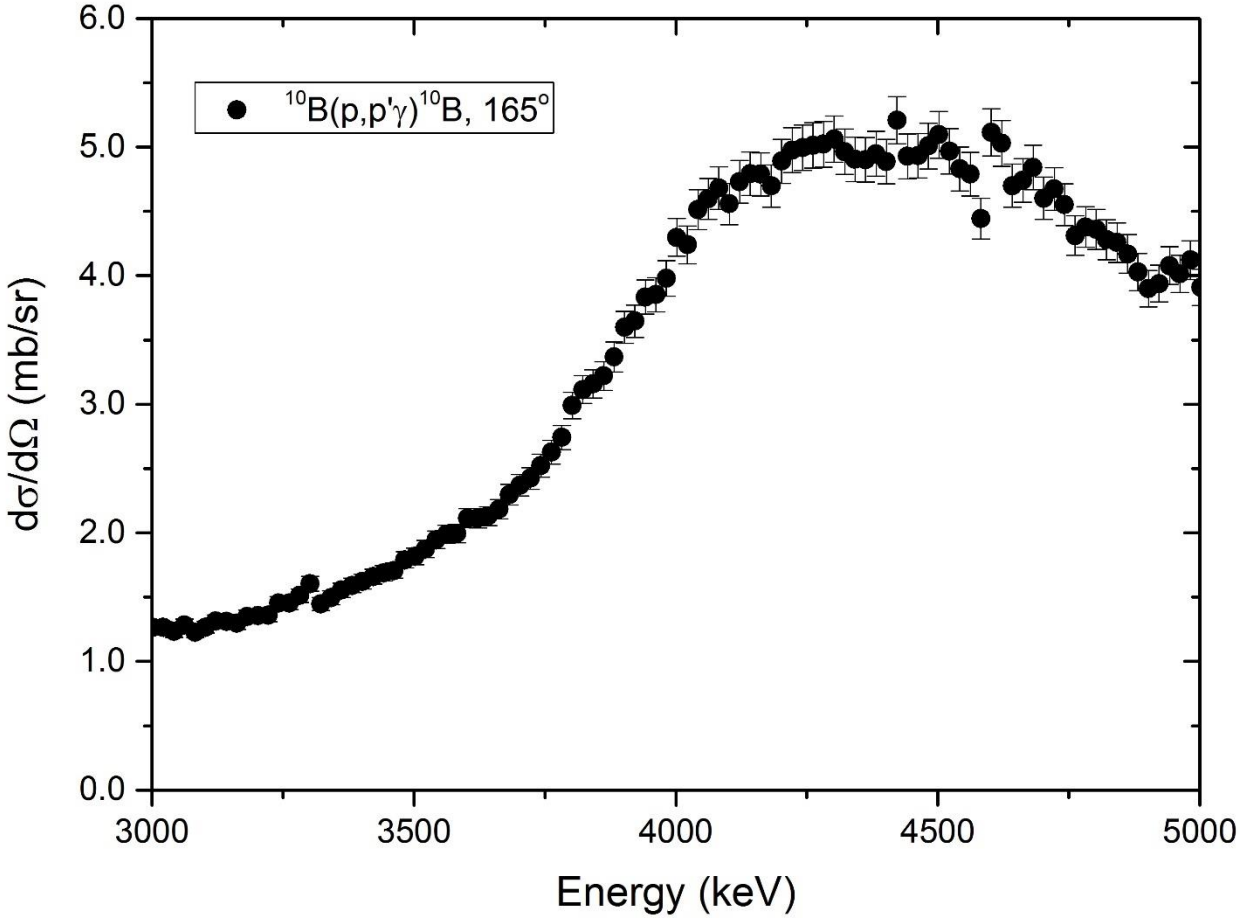

Figure 2. Simulation 1-a: slowly changing cross section, monoelemental target, no straggling, for reaction $^{10}B(p,p'\gamma)^{10}B$ at 165º.
a) Yield calculated by all codes. b) Results for all codes, shown as ratio to the average of the four calculations.

a). New figure to be made

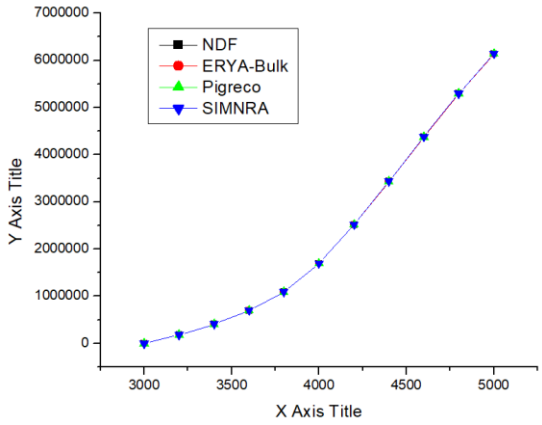

b)

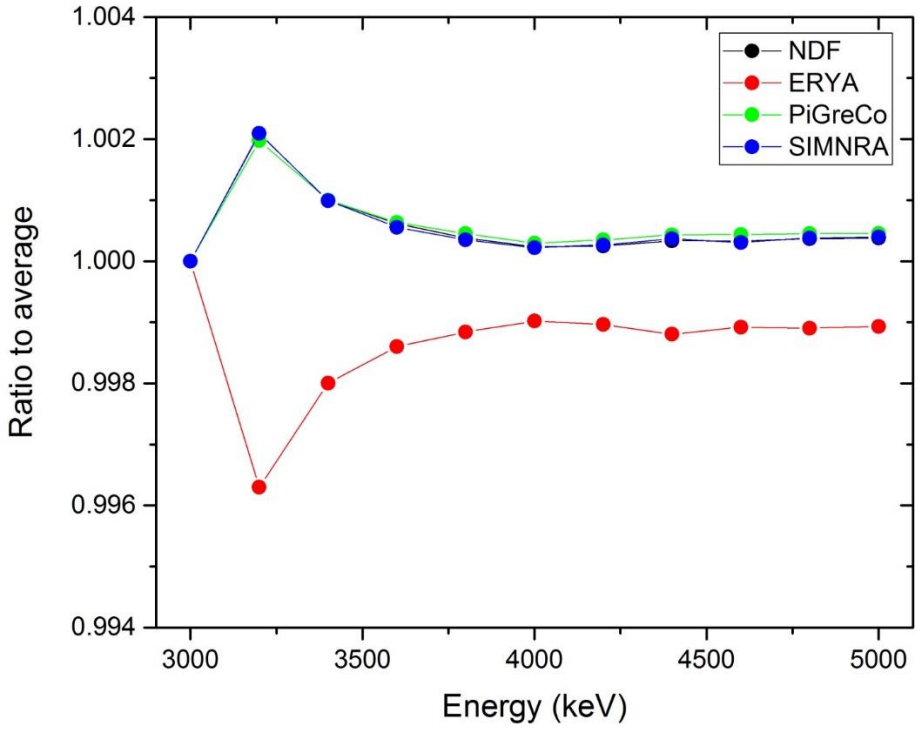

Figure 3. Simulation 1-b: slowly changing cross section, multielemental target, no straggling for reaction $^{10}B(p,p'\gamma)^{10}B$ at 165º.

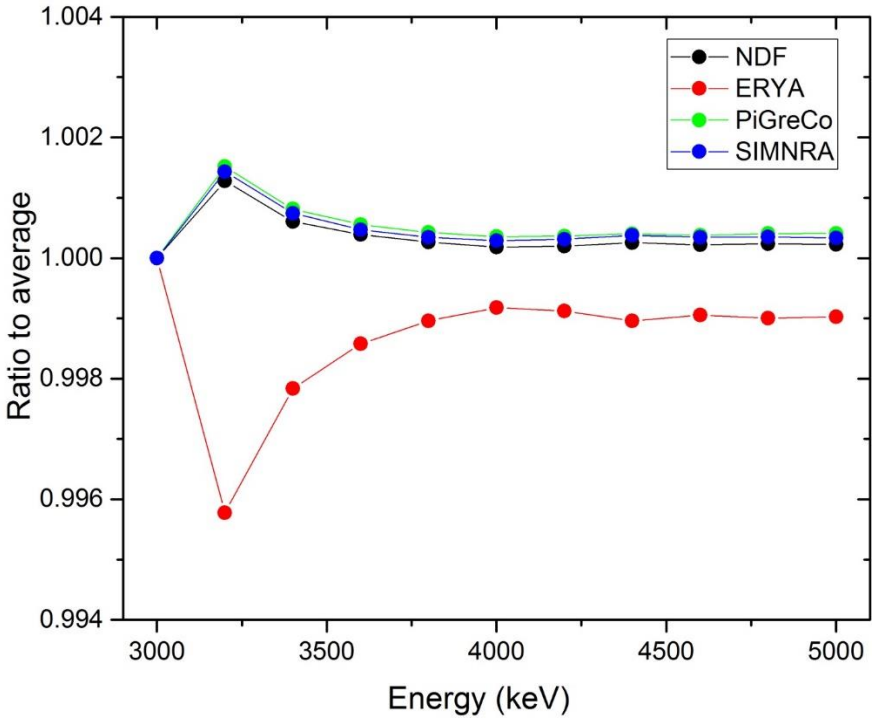
1.004
1.002
1.000
0.998
0.996
0.994
Ratio to average
3000
3500
4000
4500
5000
Energy (keV)
NDF
ERYA
PiGreCo
SIMNRA

Figure 4. Cross section for reaction $^{10}B(p,\alpha\gamma)^{7}Be$ at 150° [27].

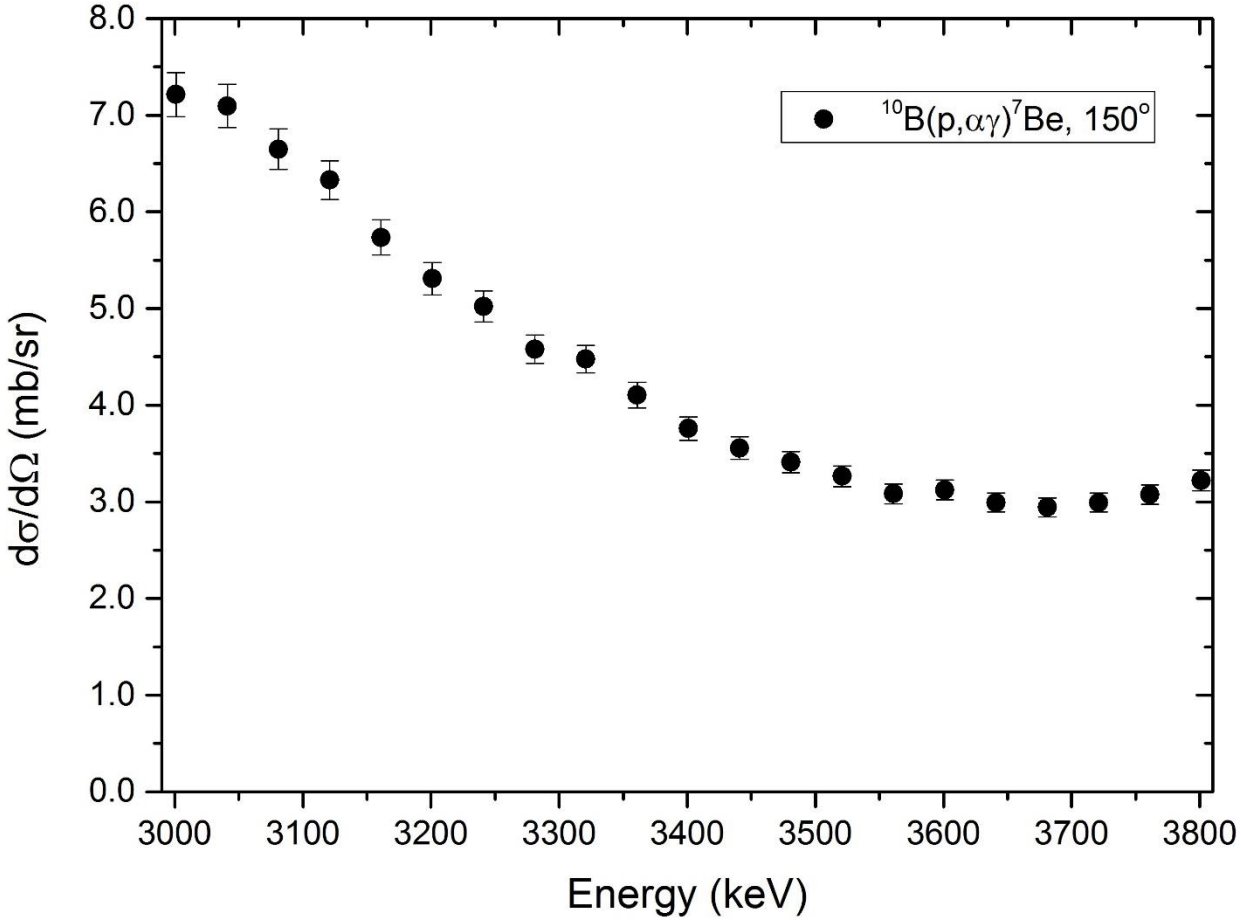

Figure 5. Simulation 2-a-i: Slowly changing cross section, monoelemental target, defined initial yield, no straggling, for reaction $^{10}B(p,\alpha\gamma)^{7}Be$ at 150º.

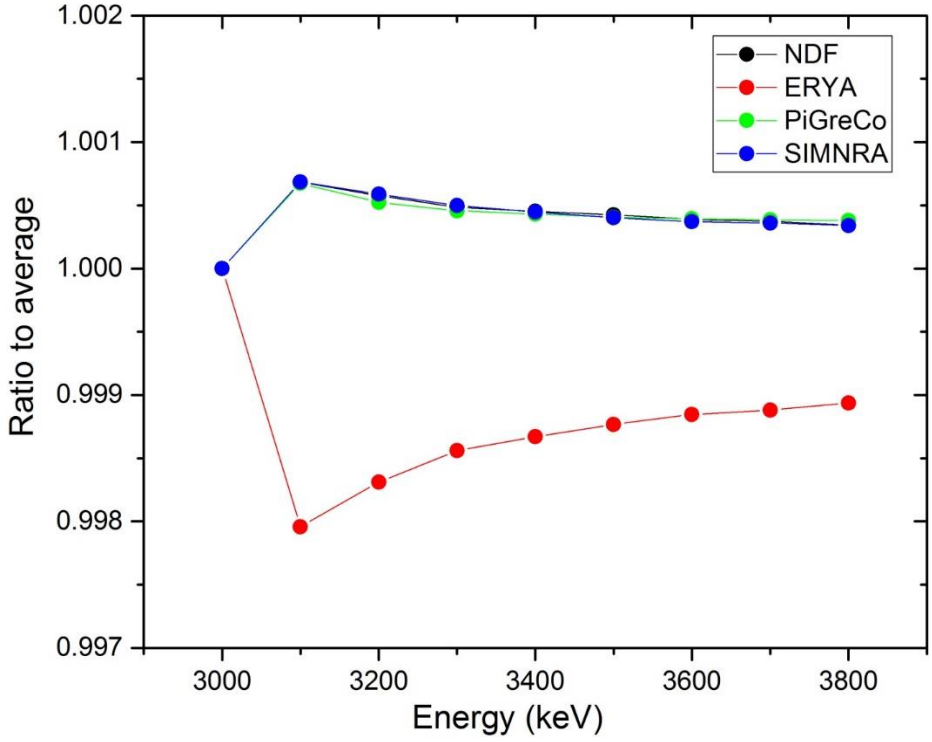

Figure 6. Simulation 2-b-i: Slowly changing cross section, monoelemental target, defined initial yield, no straggling, for reaction $^{10}B(p,p'\gamma)^{10}B$ at 165º.

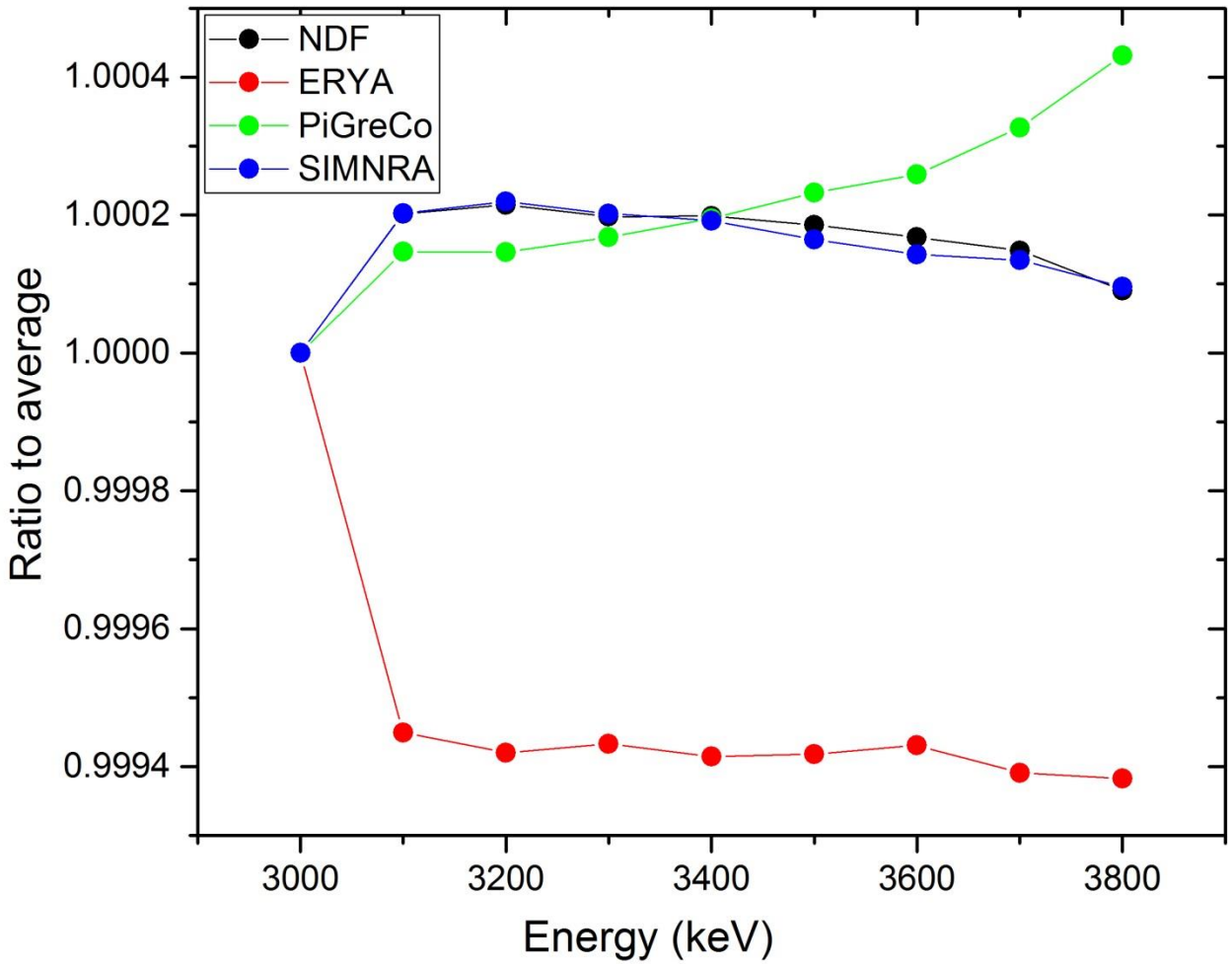

Figure 7. Simulation 2-a-ii: Slowly changing cross section, multielemental target, defined initial yield, no straggling, for reaction $^{10}B(p,\alpha\gamma)^{7}Be$.

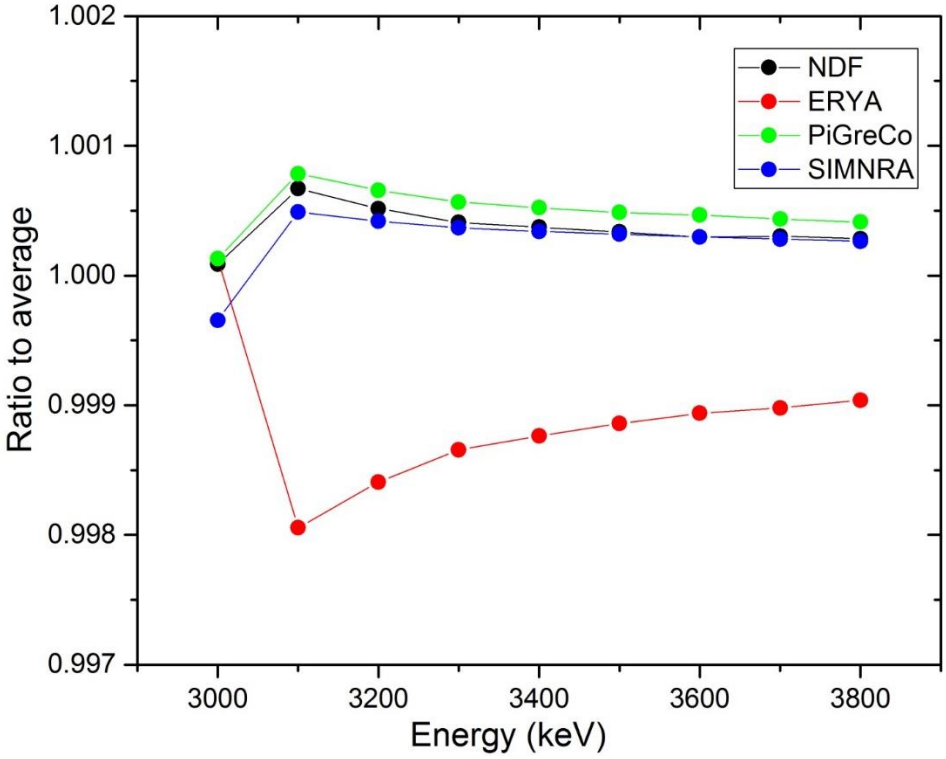

Figure 8. Simulation 2-b-ii: Slowly changing cross section, multielemental target, defined initial yield, no straggling, for reaction $^{10}B(p,p'\gamma)^{10}B$.

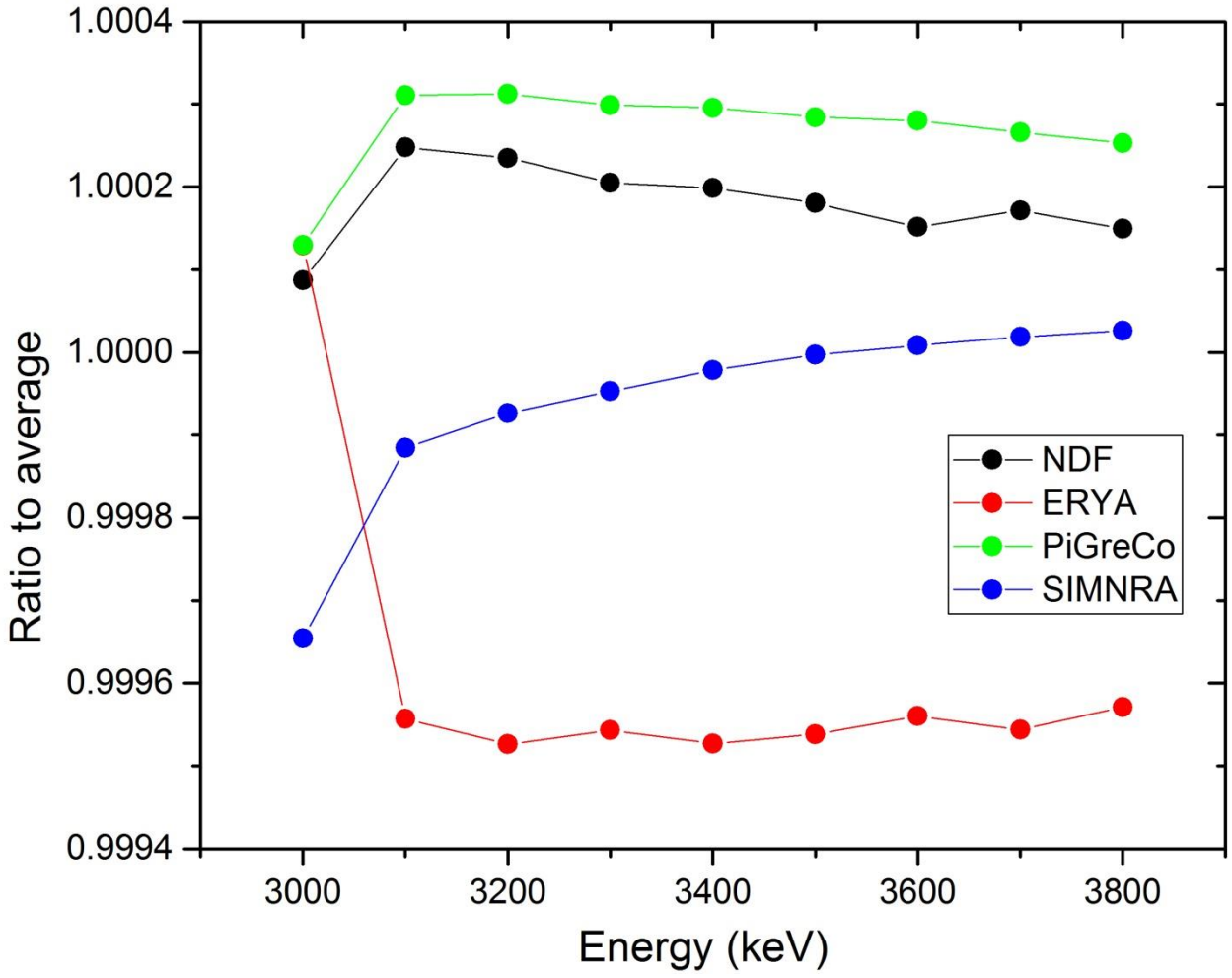

Figure 9. Cross section for reaction $^{19}F(p,p\gamma_2)^{19}F$ at 130º [28].

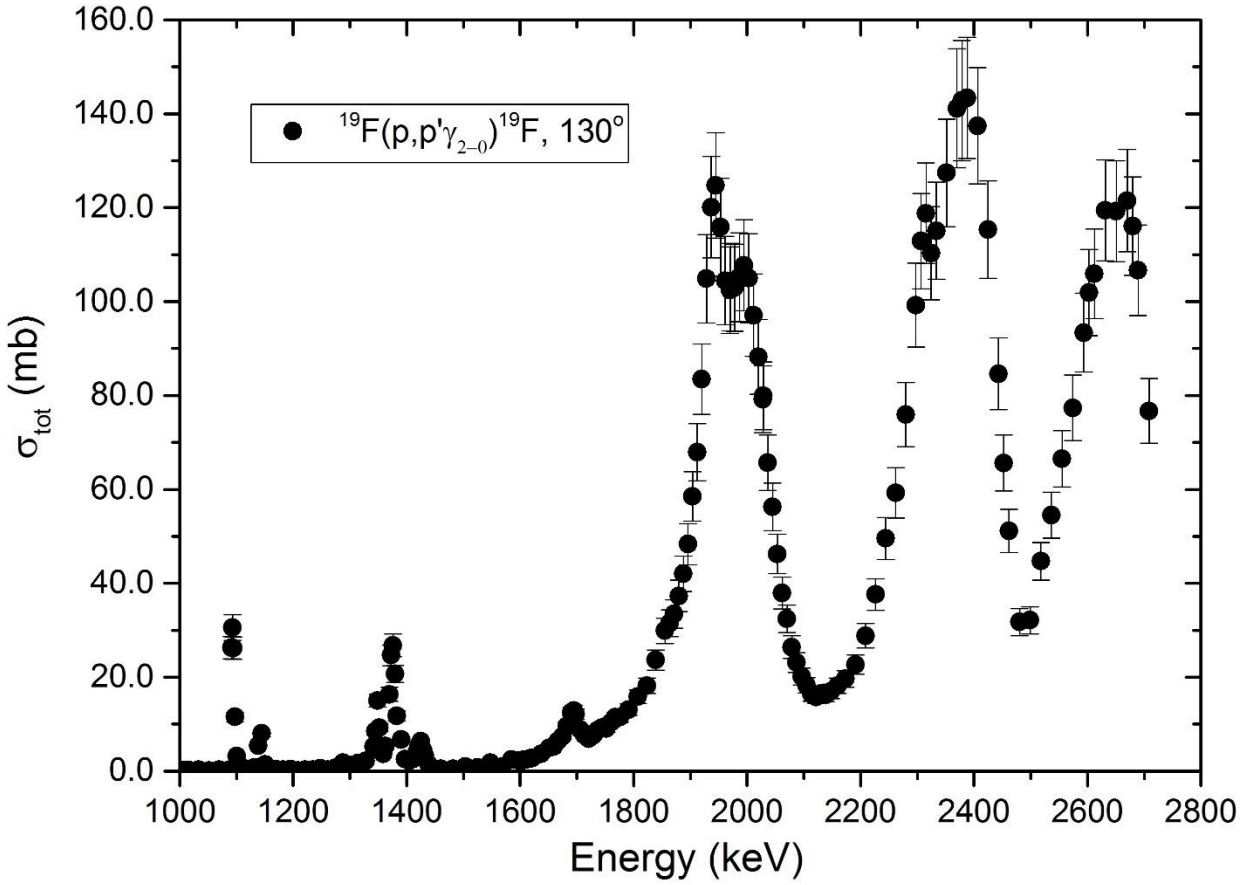

Figure 10. Simulation 3-a: Cross section with resonances, monoelemental target, no straggling, for reaction $^{19}F(p,p\gamma_2)^{19}F$ at 130º. a) Results for all codes. b) Results for all codes in the energy range 1000-1010 keV. c) Results for all codes in the energy range 1065-1105 keV. d) Results for all codes in the energy range 1065-1105 keV, shown as yield difference towards NDF. e) Results for all codes in the energy range 1300-1500 keV.

a)

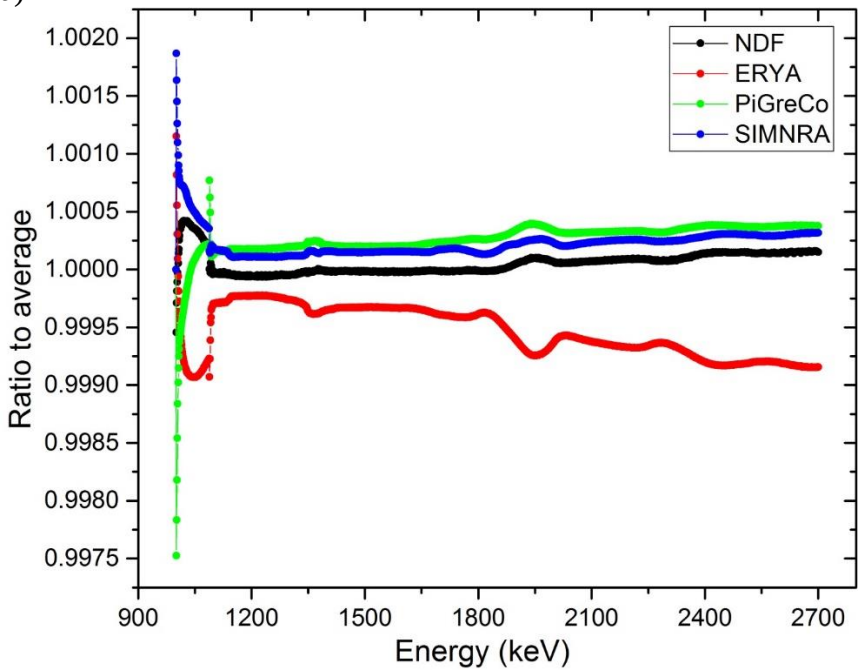

b)

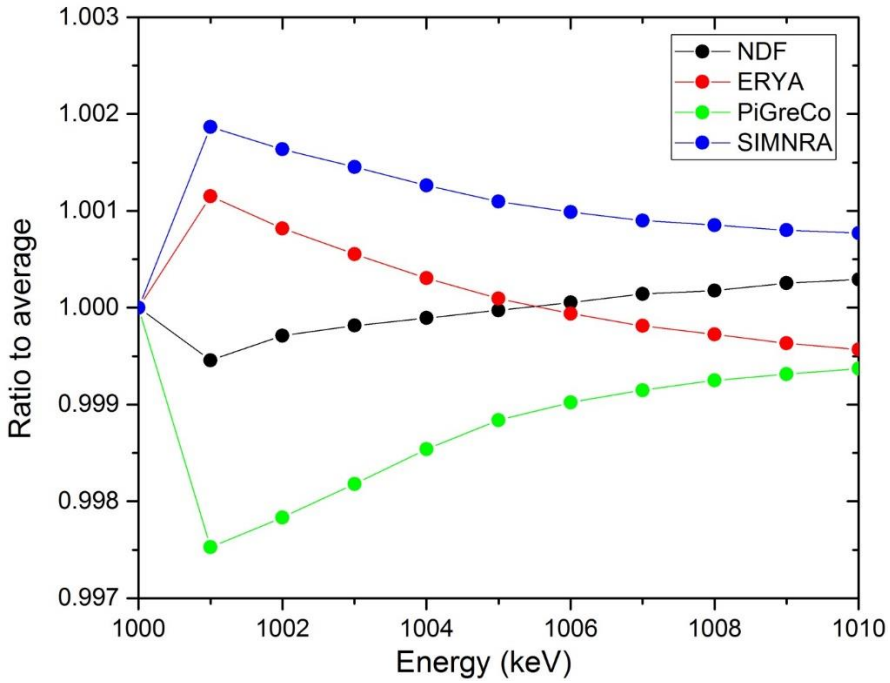

c)

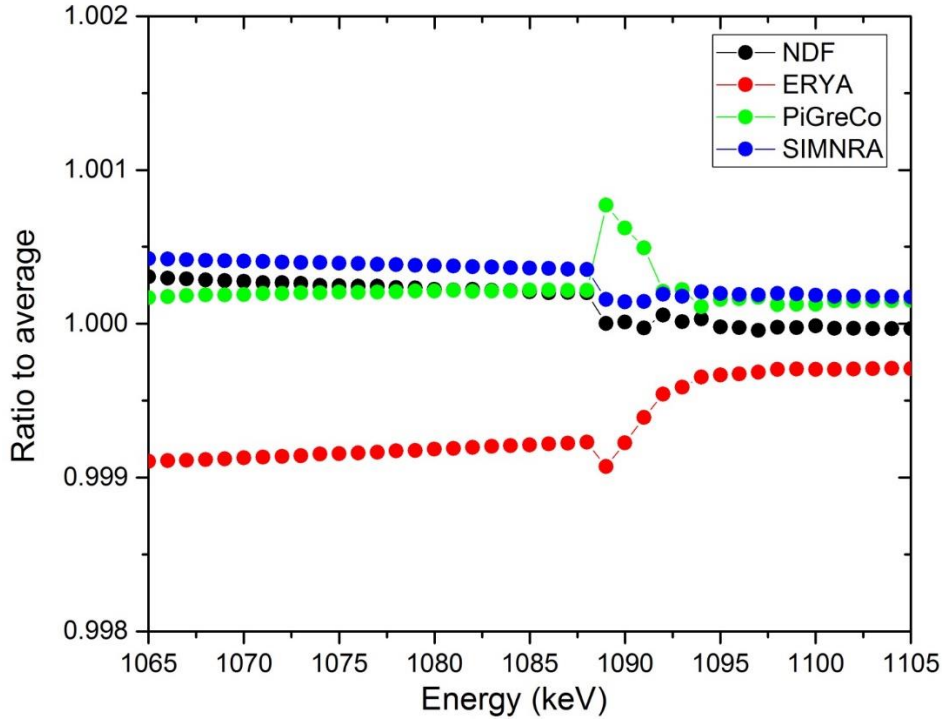
NDF
ERYA
PiGreCo
SIMNRA
Ratio to average
Energy (keV)
1.002
1.001
1.000
0.999
0.998
1065
1070
1075
1080
1085
1090
1095
1100
1105

d)

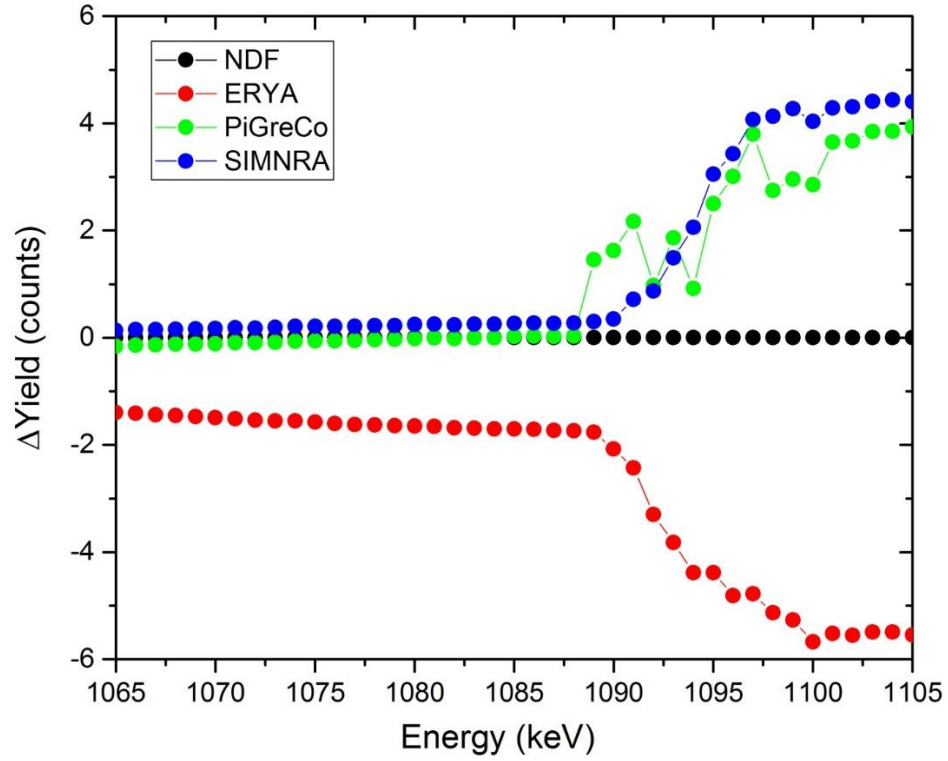
NDF
ERYA
PiGreCo
SIMNRA
ΔYield (counts)
Energy (keV)
6
4
2
0
-2
-4
-6
1065
1070
1075
1080
1085
1090
1095
1100
1105

e)

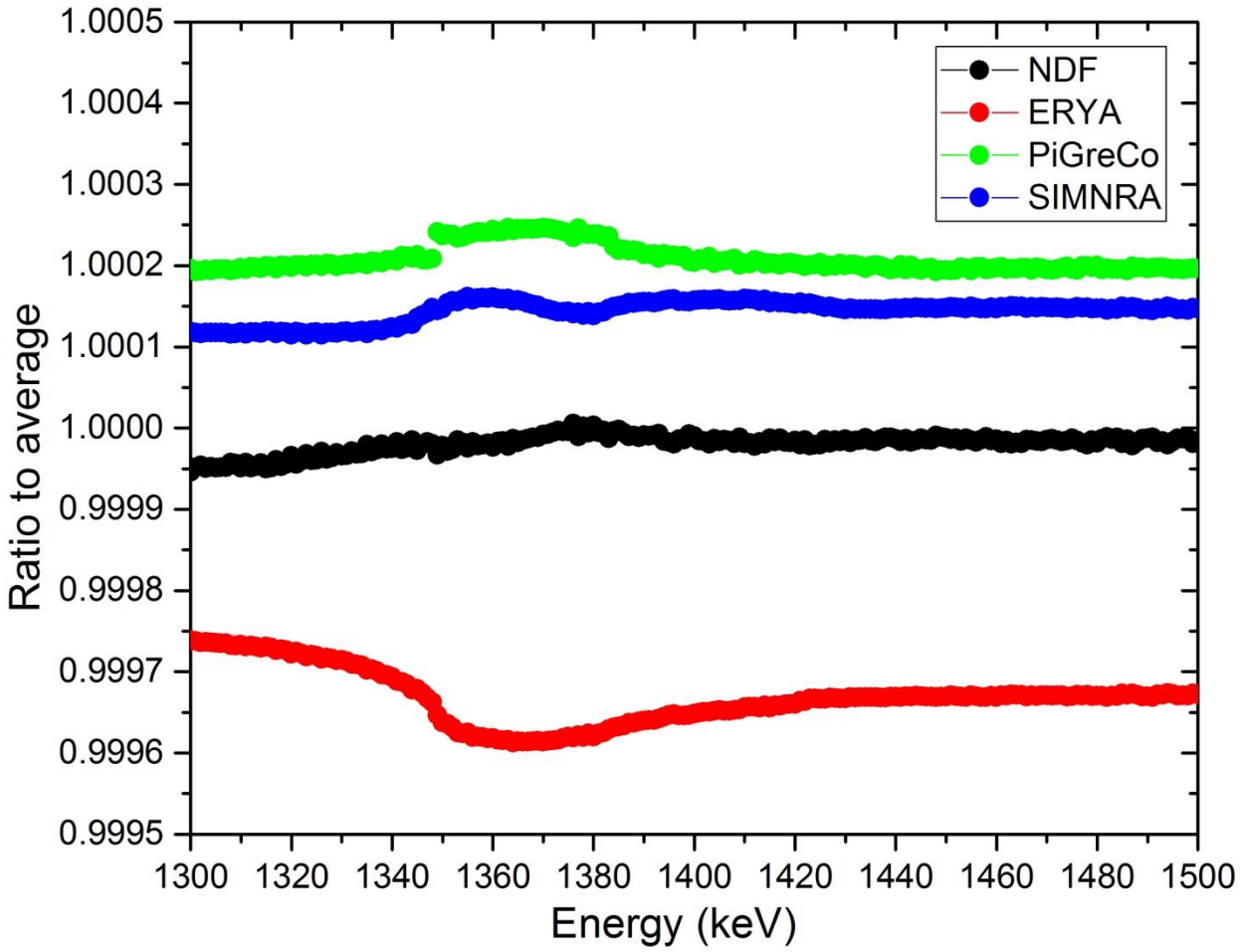
NDF
ERYA
PiGreCo
SIMNRA
Ratio to average
Energy (keV)
1.0005
1.0004
1.0003
1.0002
1.0001
1.0000
0.9999
0.9998
0.9997
0.9996
0.9995
1300
1320
1340
1360
1380
1400
1420
1440
1460
1480
1500

Figure 11. Simulation 3-b: Cross section with resonances, multielemental target, no straggling, for reaction $^{19}F(p,p\gamma_2)^{19}F$ at 130º.

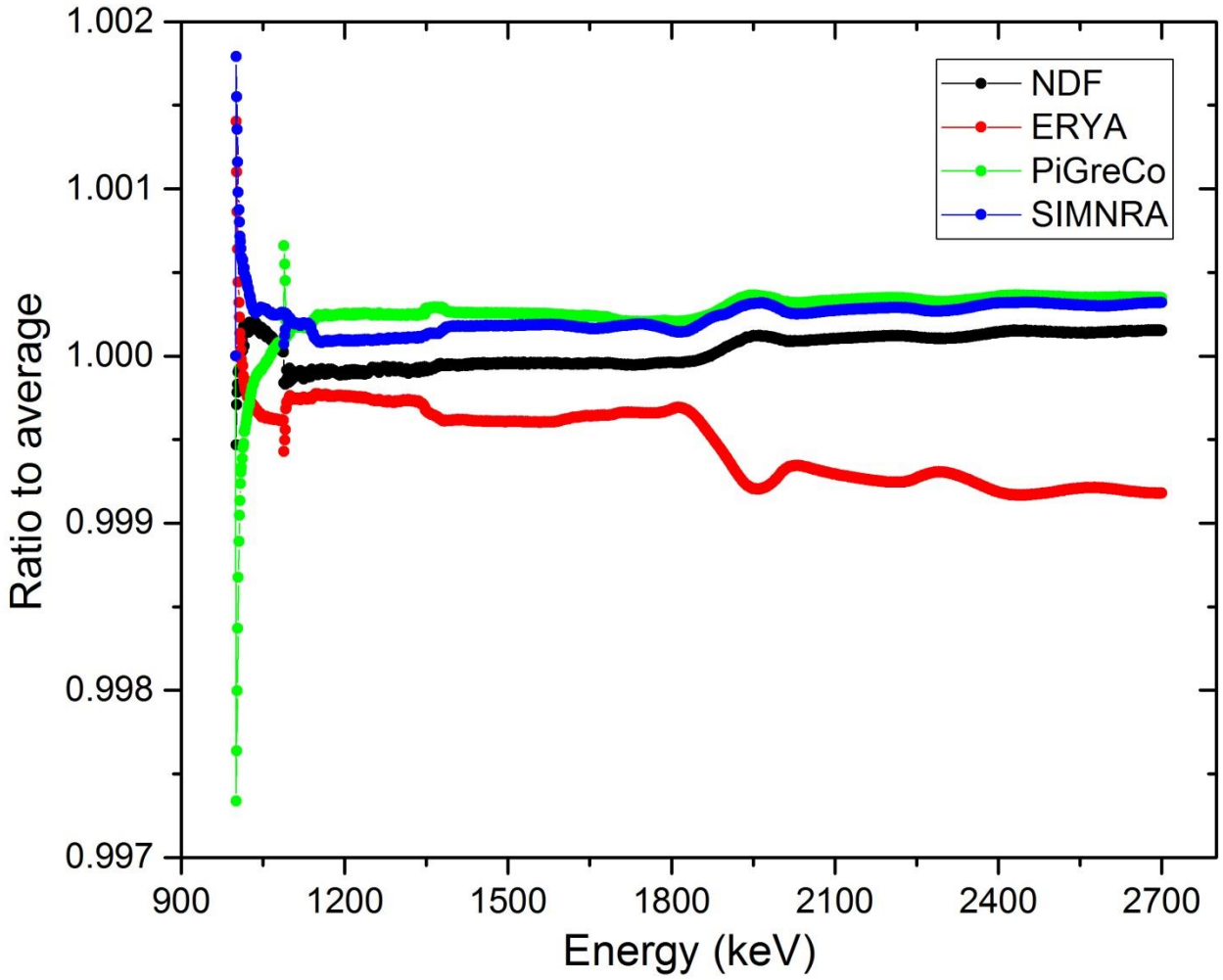

Figure 12. Simulation 4-1-a: slowly changing cross section, monoelemental target, with beam energy spread and straggling, for reaction $^{10}B(p,p'\gamma)^{10}B$ at 165º.

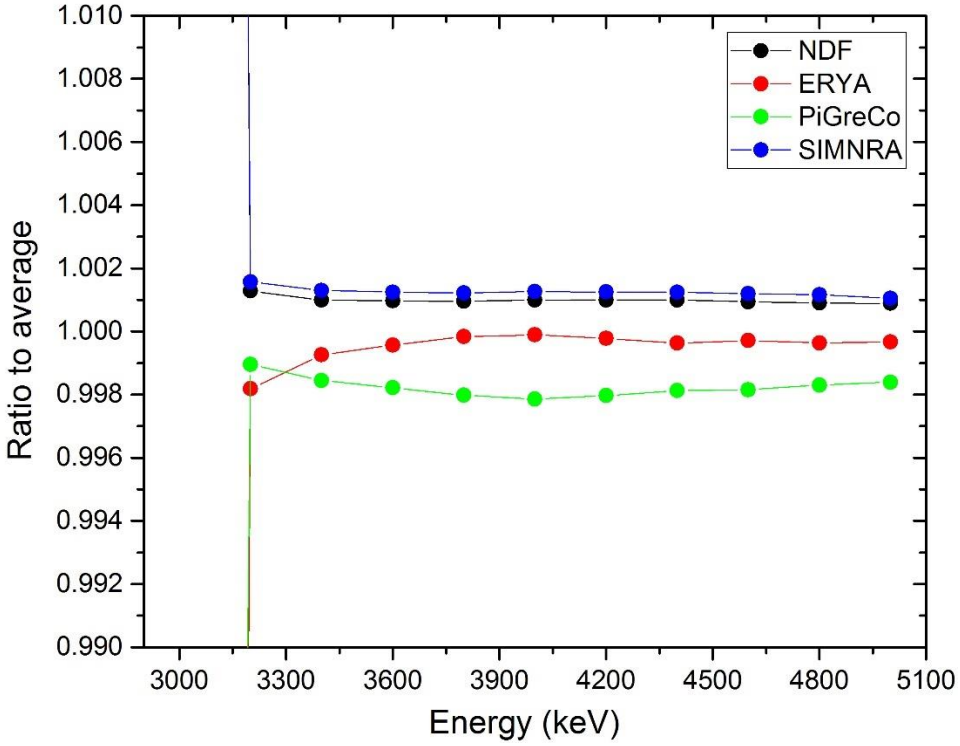

Figure 13. Simulation 4-3-a: Cross section with resonances, monoelemental target, with beam energy spread and straggling, for reaction $^{19}F(p,p\gamma_2)^{19}F$ at 130º. a) Results for all codes. b) Results for all codes in the energy range 1150-2700 keV. c) Results for all codes in the energy range 1085-1105 keV shown as calculated yield.

a)

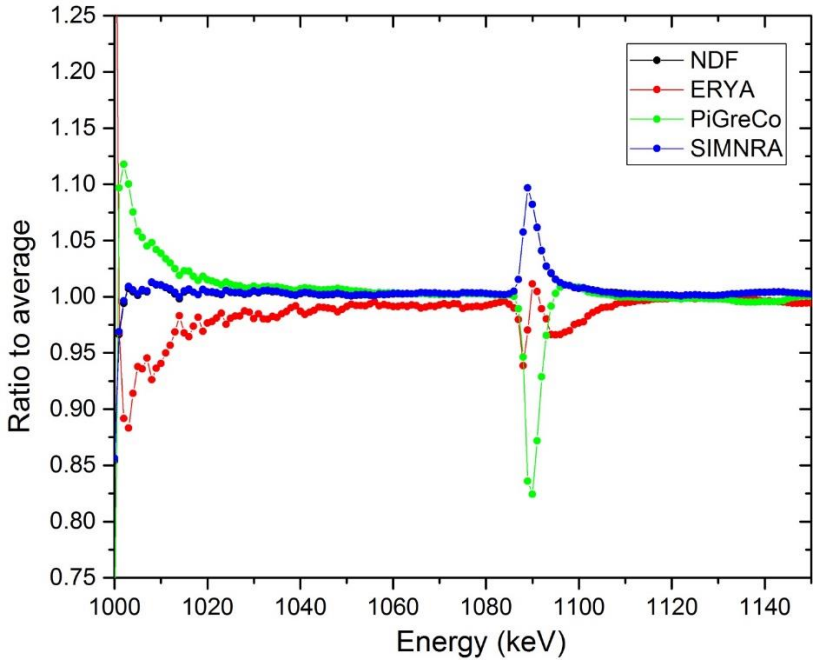

b)

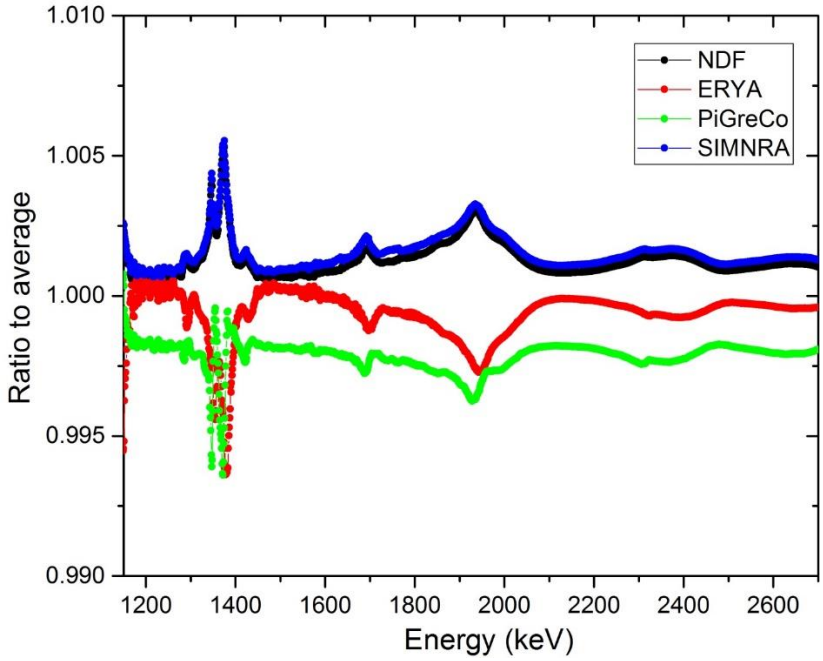

c)

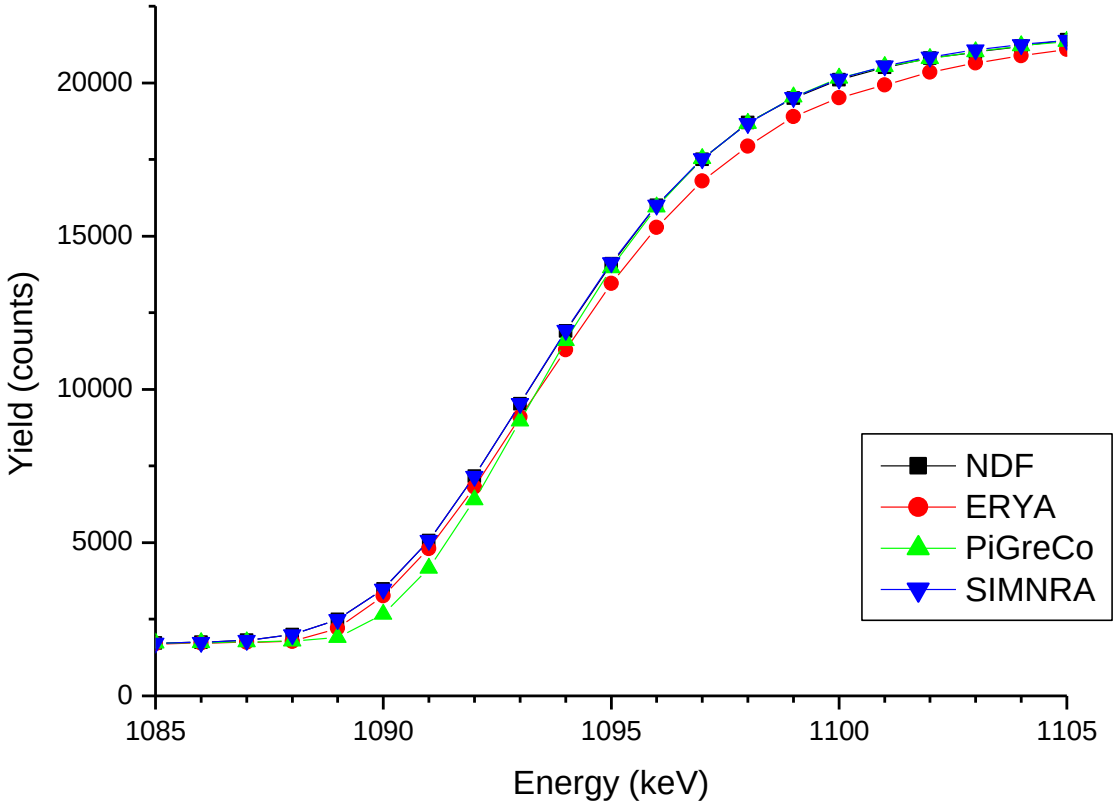
Yield (counts)
20000
15000
10000
5000
0
1085
1090
1095
1100
1105
Energy (keV)
NDF
ERYA
PiGreCo
SIMNRA